Journal of Chromatography, 607 (1992) 119–125
Elsevier Science Publishers B.V., Amsterdam

CHROM. 24 326

Noise and detection limits of indirect absorption detection in capillary zone electrophoresis

Tiansong Wang and Richard A. Hartwick

Department of Chemistry, State University of New York at Binghamton, Binghamton, NY 13902 (USA)

(First received March 6th, 1992; revised manuscript received May 6th, 1992)

ABSTRACT

The factors which contribute to the noise and signal in indirect absorption detection in capillary zone electrophoresis are studied. Two independent noise sources, the visualization agent and the detector, are distinguished. The noise from the visualization agent can be affected by the applied voltage, the surface modification of capillaries and the concentration of the visualization agent. A new factor named the "noise coefficient" is found which represents the contribution to the noise from the visualization agent. The physical interpretation of the noise coefficient is the ratio of the concentration fluctuation to the concentration of the visualization agent. A new equation that correlates detection limits with molar absorptivity and concentration of the visualization agent, noise coefficient and instrument noise is proposed, and the functions of those factors are discussed.

INTRODUCTION

Capillary zone electrophoresis (CZE) is a separation technique characterized by high efficiency and small sample volume, and great progress has been made in instrumentation and applications in the last several years. In principle, CZE is very suitable for the analysis of small ionic compounds such as aliphatic carboxylic acids, amino acids and inorganic acids. However, many of these classes of compounds lack chromophores at useful wavelengths, or have such low molar absorptivities as to preclude sensitivity by absorption detection. Conductivity detectors [1–7] and amperometric detectors [7–9] have been developed for CZE analysis of these compounds. The performance of conductivity and amperometric detectors are generally excellent, with detection limits of 10^{-6}–10^{-7} M for carboxylic acids or amino acids. However, these detectors are more difficult to fabricate than absorption detectors, and are not yet commercially available.

Correspondence to: Dr. R. A. Hartwick, Department of Chemistry, State University of New York at Binghamton, Binghamton, NY 13902, USA.

An alternative strategy to detect UV-transparent compounds in CZE is that of indirect fluorescence of indirect absorption detection. To achieve such indirect detection, an ion with either fluorescence or UV absorption properties, which is called the visualization agent, is added to the mobile phase in order to create a high background signal. The analyte ions that have the same sign of charge as the visualization agent but have no fluorescence or absorption are observed from the reduction of the background signal. Indirect fluorescence detection was first introduced to CZE by Kuhr and Yeung [10], and has been applied to the analysis of amino acids, nucleotides, inorganic anions and sugars [10–13]. Impressive detection limits can be achieved, with concentration limits of $2 \cdot 10^{-7}$ M for $H_2PO_4^-$ being reported [12].

Indirect absorption detection in CZE was first reported by Hjertén *et al.* [14]. Foret *et al.* [15] presented more details about indirect absorption detection in CZE. They observed the effect of ion mobility on the peak shape and found that higher sensitivity could be obtained by selecting visualization agents which have high molar absorptivity and effective mobilities similar to those of sample ions.

0021-9673/92/$05.00

More recently, indirect UV detection has successfully been applied to the detection of 30 anions separated by CZE [16], demonstrating great advantages over ion chromatography in terms of speed and peak capacity.

In this paper, the factors which contribute to the noise and signal in indirect absorption detection were studied, and a factor named the "noise coefficient" was defined as one of important parameters to estimate detection limit and to select operating conditions.

EXPERIMENTAL

Instrumentation

A Spectra Phoresis 1000 with SP4400 integrator (Spectra-Physics, Reno, NV, USA) was used. The fused-silica capillary (Polymicro Technologies, Phoenix, AZ, USA) was 75 μm I.D. × 360 μm O.D. with an effective length of 35.0 cm and a total length 42.5 cm. The column temperature was 25.0°C. The detector wavelength was set according to the maximum absorption position of each visualization agent. Sample was injected by 1.0-s hydrodynamic injection. A laboratory-constructed CZE apparatus was employed to conduct the noise measurement with a Pyrex rectangular capillary (0.05 × 0.5 mm, Wilmad Glass, Buena, NJ, USA). The rectangular capillary was glued to a modified cell on a Spectra 100 detector (Spectra-Physics), and an aperture of about 1.2 × 0.4 mm was created. In order to avoid the effect of light, this apparatus was operated in a dark room.

The PEG 8M-10-modified capillary was produced in our laboratory according to the temperature protocols recommended by Innophase (Portland, CT, USA).

Procedures

Capillaries were initially washed with 1 *M* NaOH for 10 min, except the PEG-modified column, then washed with water. In most of cases, the capillaries were equilibrated with buffer overnight. The detector noise (peak-to-peak) was measured with capillaries filled with buffer (*i.e.*, the visualization agent solution) and without voltage. The total noise was measured from a 2–3 min segment of a stable baseline while a certain voltage was applied.

Stock solutions of 50 m*M* 4-nitrophenol (NPH), 10 m*M* 1,3,5-benzenetricarboxylic acid (BTA) and 2 m*M* 1-naphthylacetic acid (NAA) were prepared by dissolving the chemicals in boiling pure water (17 MΩ). After cooling, the final volume was adjusted and the solution was filtered through a 0.45-μm membrane. Lower concentration solutions were obtained by dilution. pH 4 buffers were made by adding NaOH solution or Tris solution, pH 8 buffers by adding Tris solution–Tris solid.

Propionic acid and hexanoic acid solutions ($1.1 \cdot 10^{-2}$ *M* each) were prepared and adjusted to pH 4.1 or 8.0 by Tris solution in order to keep the sample pH close to the buffer pH, then diluted to the desired concentration with distilled water. Just before injection, the sample solutions were further diluted with buffer at a 1:1 ratio, and the indicated concentration was that after dilution with buffer.

Chemicals

BTA, NPH, NAA and hexanoic acid were obtained from Aldrich (Milwaukeek, WI, USA), PEG 8M-10 from Innophase, Tris from Bio-Rad Labs. (Richmond, CA, USA) and all other chemicals from Fisher (Fair Lawn, NJ, USA).

RESULTS AND DISCUSSION

Noise from visualization agent

For indirect fluorescence and indirect absorption detection, the major factors determining the detection limits have been reported to be the concentration of the visualization agent, C_v, the dynamic reserve, D_r (*i.e.*, the ratio of the background absorbance to the noise), and the displacement ratio, R (*i.e.*, the number of visualization agent molecules transferred by one analyte molecule) [17–20]. The detectable concentration, C_{det}, can be estimated from eqn. 1 [17]:

$$C_{det} = C_v/(RD_r) \quad (1)$$

According to eqn. 1, lowering C_v and increasing D_r will reduce the detection limit. However, there are two questionable points in eqn. 1. First, it has been found that the D_r value somehow depends on C_v [17,19]. Therefore, one may not reduce detection limits according to eqn. 1 by lowering C_v, because D_r is reduced simultaneously. Secondly, in eqn. 1, the function of molar absorptivity of the visualization agent is not clear, although some authors

TABLE I

RELATIONSHIP OF NOISE TO VISUALIZATION AGENT CONCENTRATION IN A ROUND CAPILLARY

Conditions: 75 μm I.D. fused-silica capillary; BTA–NaOH buffer, pH 4.22; 355 V/cm.

C_v (mM)	Background (a.u.)	Slope (a.u./mM)[a]	σ_v ($\times 10^{-5}$)	K_n ($\times 10^{-15}$)
0.40	0.072	0.162	0.47	7.2
1.00	0.162	0.135	1.2	8.9
2.00	0.275	0.095	1.6	8.4
4.00	0.403	0.038	1.5	9.8

[a] Tangent of the regression curve at each concentration.

[19,20] recommend the use of visualization agent with high molar absorptivity.

In this research, it is found that the noise in indirect absorption detection includes at least two sources: the visualization agent and the detector (electronic, source, etc.). From the viewpoint of absorption measurements [21], noise is the unwanted fluctuations in the desired signal, and the noise magnitudes are typically expressed as either root-mean-square (rms) or peak-to-peak (p–p) values. Since the square values of independent rms noises are additive, for indirect absorption detection in CZE, we have

$$\sigma_{tot}^2 = \sigma_v^2 + \sigma_d^2 \quad (2)$$

where σ_{tot} is the total rms noise, σ_v the rms noise from the visualization agent and σ_d the rms noise from the detector. In experiments, the peak-to-peak noise is more easily to be measured, with the rms noise being approximately one fifth of the p–p noise [21]. Therefore,

$$(5\sigma_{tot})^2 = (5\sigma_v)^2 + (5\sigma_d)^2 \quad (3)$$

or

$$N_{tot}^2 = N_v^2 + N_d^2 \quad (4)$$

where N_{tot} is the total p–p noise, N_v the p–p noise from the visualization agent and N_d the p–p noise from the detector.

The noise measurements indicate that, when keeping the voltage constant, the σ_v value varies with the visualization agent, as it is seen from Tables I and II. However, between concentration and noise, there is a factor, K_n, which remains approximately constant, and a new relationship can be established as follows:

$$\sigma_v = K_n C_v S_p \quad (5)$$

where K_n is named the noise coefficient, and S_p is the slope of concentration *versus* absorbance. Within the linear range, S_p is equal to εb, where ε is molar absorptivity and b is the equivalent optical path length of capillary. In Table I (round capillary), the K_n values of BTA fall between $7.2 \cdot 10^{-5}$ and $9.8 \cdot 10^{-5}$, which are approximately a constant within the measurement error. It is also noticed that the calibration curve using the round capillary is not linear (non-constant slopes in Table I), which may interfere the measurement. In order to eliminate any possible effect due to the deviations from Beer's law, the noise measurement was performed using a rectangular capillary, which gave an excellent straight line in the concentration *versus* absorbance plot, and the K_n values of NPH fall between $3.2 \cdot$

TABLE II

RELATIONSHIP OF NOISE TO VISUALIZATION AGENT CONCENTRATION IN A RECTANGULAR CAPILLARY

Conditions: 0.05 × 0.5 mm Pyrex rectangular capillary; NPH–Tris buffer, pH 8.29; 200 V/cm.

C_v (mM)	Background (a.u.)[a]	N_{tot} (10^{-4} a.u.)	N_d (10^{-4} a.u.)	σ_v (10^{-4} a.u.)	K_n ($\times 10^{-4}$)
1.0	0.074	3.6	3.6	–	–
3.0	0.224	7.2	5.2	1.0	4.4
6.0	0.448	12	9.2	1.5	3.3
15.0	1.136	43	39	3.6	3.2

[a] Constant slope (0.0075 a.u./mM) from the regression equation.

10^{-4} and $4.4 \cdot 10^{-4}$ (Table II). These data indicate that in each case K_n is approximately a constant.

A very important phenomenon observed in the noise measurement is that the N_{tot} values are obviously affected by the applied voltage, both in rectangular and round capillaries. Assuming the N_d remains constant during voltage changes, the σ_v, then the K_n values, according to eqns. 4 and 5, respectively, will be affected by the applied voltage. One of the changes of K_n values is presented in Fig. 1. The changes of N_{tot} values with the electric field strength indicate that the noise contribution from the visualization agent is not caused by the absorbance measurement such as the source fluctuation, but presumably caused by the concentration fluctuation.

In order to determine what factors are responsible for the additional noise, the noise was measured under different pH values and different columns, and the results are tabulated in Table III. It is found that using BTA–Tris buffer, the noise contribution from the visualization agent is almost undetectable in the PEG-bonded capillary. The dramatic reduction in noise when using a PEG capillary was unexpected, and the results suggest that interactions such as adsorption between the visualization agent and the capillary wall could be responsible for the noise. If adsorption is one of the reasons leading to extra noise in a bare silica capillary, a higher pH value would lead to lower noise, due to enhanced repulsion between the BTA and the silica surface in basic buffers. This inference has been verified experimentally. The data in Table III demonstrated that when the pH is increased from 4.25 to 8.25, the σ_v value is decreased from $1.3 \cdot 10^{-5}$ to $0.57 \cdot 10^{-5}$ a.u., and the K_n value is simultaneously reduced from $4.6 \cdot 10^{-5}$ to $2.0 \cdot 10^{-5}$.

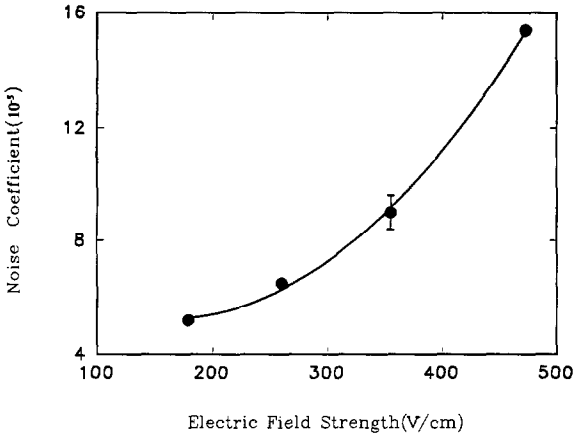

Fig. 1. Relationship of the noise coefficient to the electric field strength. Conditions: 75 μm I.D. × 360 μm O.D. fused-silica capillary; 2.0 m*M* BTA–NaOH buffer, pH 4.22; detector wavelength 210 nm; rise time 0.5 s. The bar represents the range of three measurements in different days.

Based on the results mentioned above, it is reasonable to assume that σ_v is created by the concentration fluctuation of the visualization agent, ΔC_v, although it is hard to tell how such a fluctuation is generated. Thus,

$$\sigma_v = \Delta C_v S_p \quad (6)$$

Combining eqns. 5 and 6, we have

$$K_n = \Delta C_v / C_v \quad (7)$$

Eqn. 7 suggests the physical meaning of the noise coefficient: the ratio of concentration fluctuation to concentration of the visualization agent. Different visualization agents may have different K_n values. K_n is independent of the concentration of the visualization agent, but is dependent on the applied voltage and surface chemistry of capillaries.

TABLE III

EFFECT OF pH AND SURFACE MODIFICATION ON THE NOISE COEFFICIENT

Column[a]	Conditions	σ_v (10^{-5} a.u.)	K_n ($\times 10^{-5}$)
Bare	2 m*M* BTA–Tris, pH 4.25; 306 V/cm	1.3	4.6
PEG-bonded	2 m*M* BTA–Tris, pH 4.21; 306 V/cm	<0.2	<0.7
Bare	2 m*M* BTA–Tris, pH 8.25; 306 V/cm	0.57	2.0

[a] All are 75 μm I.D. fused-silica capillaries.

Detection limit

The detection limit depends on the signal-to-noise (S/N) ratio. Ideally, the signal in indirect absorption detection is

$$\Delta A = (R\varepsilon_v - \varepsilon_s)bC_s \quad (8)$$

where ΔA is the reduction of background absorbance, R is the displacement ratio (the number of visualization agent molecules transferred by one analyte molecule), ε_s and ε_v are the molar absorptivity of the sample and the visualization agent, respectively, b is the equivalent optical path length of the capillary and C_s is the sample concentration. When the molar absorptivity of the analyte is much smaller than that of the visualization agent, $R\varepsilon_v - \varepsilon_s \approx R\varepsilon_v$, thus

$$\Delta A = R\varepsilon_v bC_s \quad (9)$$

Combining eqns. 4, 5 and 9 (within the linear range, $S_p = \varepsilon_v b$), we have

$$S/N = \left[\frac{\Delta A^2}{N_{tot}^2}\right]^{0.5} = \left[\frac{(R\varepsilon_v bC_s)^2}{(5\,K_n C_v \varepsilon_v b)^2 + N_d^2}\right]^{0.5} \quad (10)$$

The detection limit, C_{lim}, is usually measured at an S/N of 3, thus

$$C_{lim} = C_s = 3\left[\frac{(5\,K_n C_v \varepsilon_v b)^2 + N_d^2}{(R\varepsilon_v b)^2}\right]^{0.5} \quad (11)$$

In practice, $\varepsilon_v b$ may be replaced by the real slope, thus

$$C_{lim} = 3\left[\frac{(5\,K_n C_v \varepsilon_v b)^2 + N_d^2}{(RS_p)^2}\right]^{0.5} \quad (12)$$

Eqn. 11 indicates that ε_v contributes both signal and noise; simply selecting visualization agents with higher ε_v may not necessarily lead to lower detection limits. There are two extreme conditions in eqn. 11.

(a) $(5K_nC_v\varepsilon_v b)^2 \gg N_d^2$: eqn. 11 becomes

$$C_{lim} \approx 15\,K_nC_v/R \quad (13)$$

The detection limit cannot be improved by increasing ε_v, but lowering C_v will reduce the detection limit. It is noticed that eqn. 13 is very similar to eqn. 1. In other words, eqn. 1 could be treated as a specific expression of eqn. 12.

(b) $(5K_nC_v\varepsilon_v b)^2 \ll N_d^2$: eqn. 11 becomes

$$C_{lim} \approx 3\,N_d/R\varepsilon_v b \quad (14)$$

Lowering V_v does not reduce detection limits any more, instead, increasing ε_v will improve detection limits.

From these extreme conditions, a reasonable inference is that combinations of high ε_v and low C_v will give a lower detection limit, and such an experimental result has been observed by Foret *et al.* [15]. However, the requirements of buffer capacity, buffer conductivity and adequate background absorbance which is corresponding to a lower detection error and falls in the linear range of the detector must be considered when one selects the values of ε_v and C_v.

The function of K_n is obvious in eqn. 11, that is, the lower the better. Since the mechanism of the concentration fluctuation is not clear at present, experimental selection of visualization agents and surface modification have to be done in order to obtain lower detection limits.

Fig. 2 illustrates the effect of ε_v on detection. The electropherograms were obtained from one injection but monitored at two wavelengths. The background absorbance ratio, which is equal to the ε_v ratio, is 5.21, and higher peaks are generated by the higher ε_v value. The peak-height ratios are 4.92–

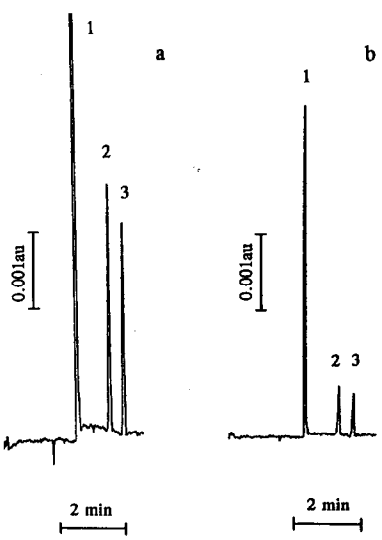

Fig. 2. Effect of the molar absorptivity of the visualization agent on detection. (a) Detector wavelength 210 nm; (b) detector wavelength 240 nm. Conditions: 75 μm I.D. × 360 μm O.D. fused-silica capillary; 0.5 mM BTA–Tris buffer, pH 8.20. Peaks: 1 = water; 2 = $5.5 \cdot 10^{-5}$ M hexanoic acid; 3 = $5.5 \cdot 10^{-5}$ M propionic acid.

4.93, quite close to the background absorbance ratio. Since the noise at 210 nm is a little higher than that at 240 nm, the calculated detection limit (S/N = 3) for propionic acid at 210 nm is only a 3.3-fold improvement compared to that at 240 nm.

Linearity of detection

The indirect absorption detection in CZE was estimated to have a narrow dynamic linear range [15], because the concentration of the analyte must be much lower than that of the buffer in order to reduce the disturbance of the local electric field. However, it has been found that the dynamic linear range depends on what parameter is measured. From Fig. 3 it is seen that the linearity in terms of peak height is poor, but the linearity in terms of peak area is very good (except the outlier at $1.1 \cdot 10^{-6}$ M) and the dynamic linear range extends at least two orders of magnitude from $3.3 \cdot 10^{-6}$ to $3.3 \cdot 10^{-4}$ M (buffer concentration is only 1 mM) with a linear regression coefficient (r^2) of 0.99996, even though the asymmetric factor of the peaks changes from 1.2 to 12.8. It should be mentioned that, although the quantitation is available at high sample concentration, the peak becomes broad and the resolving power is sacrificed. At $1.1 \cdot 10^{-6}$ M, noise obviously interferes with area integration, thus deteriorating linearity.

CONCLUSIONS

In this paper, the factors which contribute to the noise and signal in indirect absorption detection in CZE are studied. Two independent noise sources are distinguished, *i.e.*, the visualization agent and the detector. Although the mechanism of the noise from the visualization agent is not clear at present, the experimental results indicate that the noise has both chemical and physical natures, because the noise can be affected by the surface modification of a capillary and the applied voltage, as well as the concentration of the visualization agent. A new factor, named the noise coefficient, is found which represents the contribution to the noise from the visualization agent, and the coefficient is interpreted as the ratio of the concentration fluctuation to the concentration of the visualization agent. The factors that contribute to the noise and the signal are summarized in eqn. 11, and the functions of the molar absorptivity and the concentration of the visualization agent, the noise coefficient and the detector noise are discussed.

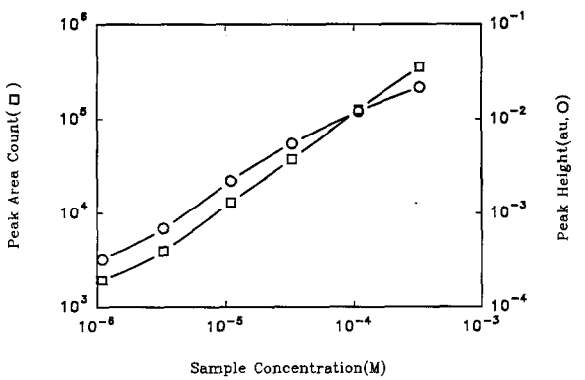

Fig. 3. Linearity of detection. Conditions: 1.0 mM NAA–Tris buffer, pH 8.09. Sample: propionic acid; 1.0-s hydrodynamic injection.

ACKNOWLEDGEMENTS

This research was supported by the Center for Biotechnology of the State University of New York at Stony Brook and by the Spectra-Physics Analytical Instrument Division.

REFERENCES

1 F. E. P. Mikkers, F. M. Everaerts and Th. P. E. M. Verheggen, *J. Chromatogr.*, 169 (1979) 11.
2 P. Gebauer, M. Deml, P. Boček and J. Janák, *J. Chromatogr.*, 267 (1983) 455.
3 J. L. Beckers, Th. P. E. M. Verheggen and F. M. Everaerts, *J. Chromatogr.*, 452 (1988) 591.
4 X. Huang, T. J. Pang, M. J. Gordon and R. N. Zare, *Anal. Chem.*, 59 (1987) 2747.
5 X. Huang, J. A. Luckey, M. J. Gordon and R. N. Zare, *Anal. Chem.*, 61 (1989) 766.
6 X. Huang, M. J. Gordon and R. N. Zare, *J. Chromatogr.*, 480 (1989) 285.
7 X. Huang, R. N. Zare, S. Sloss and A. G. Ewing, *Anal. Chem.*, 63 (1991) 189.
8 R. A. Wallingford and A. G. Ewing, *Anal. Chem.*, 60 (1988) 1972.
9 T. M. Olefirowicz and A. G. Ewing, *J. Chromatogr.*, 499 (1990) 713.
10 W. G. Kuhr and E. S. Yeung, *Anal. Chem.*, 60 (1988) 1832.
11 W. G. Kuhr and E. S. Yeung, *Anal. Chem.*, 60 (1988) 2642.
12 L. Gross and E. S. Yeung, *J. Chromatogr.*, 480 (1989) 169.
13 T. M. Garner and E. S. Yeung, *J. Chromatogr.*, 515 (1990) 639.
14 S. Hjertén, K. Elenbring, F. Kilar, J. L. Liao, A. J. C. Chen, C. J. Siebert and M. D. Zhu, *J. Chromatogr.*, 403 (1987) 47.

15 F. Foret, S. Fanali, L. Ossicini and P. Boček, *J. Chromatogr.*, 470 (1989) 299.
16 W. R. Jones and P. Jandik, *J. Chromatogr.*, 546 (1991) 445.
17 T. Takeuchi and E. S. Yeung, *J. Chromatogr.*, 370 (1986) 83.
18 W. D. Pfeffer, T. Takeuchi and E. S. Yeung, *Chromatographia*, 24 (1987) 123.
19 T. Takeuchi and D. Ishii, *J. Chromatogr.*, 393 (1987) 419.
20 D. Ishii and T. Takeuchi, *J. Liq. Chromatogr.*, 11 (1988) 1865.
21 J. D. Ingle, Jr. and S. R. Crouch, *Spectrochemical Analysis*, Printice-Hall, Englewood Cliffs, NJ, 1988, Ch. 5.